coatings

MDPI

Review

Self-Assembled Monolayer Coatings on Gold and Silica Surfaces for Antifouling Applications: A Review

Yunsoo Choi, Hung-Vu Tran and T. Randall Lee *

Department of Chemistry and the Texas Center for Superconductivity, University of Houston, 4800 Calhoun Road, Houston, TX 77204-5003, USA
* Correspondence: trlee@uh.edu

Abstract: The resistance of surfaces to biomaterial adsorption/adhesion is paramount for advancing marine and biomedical industries. A variety of approaches that involve bioinert materials have been developed to modify surfaces. Self-assembled monolayers (SAMs) are powerful platforms in which the surface composition is easily fabricated and a well-defined structure is provided; thus, the molecular-level interaction between biomolecules/biofoulants and the surface can be understood. In this review, we describe a wide variety of SAM structures on gold and silica surfaces for antifouling applications and the corresponding mechanism of nonfouling surfaces. Our analysis divides the surface properties of films into the following types: (1) hydrophilic, (2) hydrophobic, and (3) amphiphilic films.

Keywords: antifouling coatings; self-assembled monolayers (SAMs); fluorocarbon; oligo(ethylene glycol) (OEG); amphiphilic coatings; hydrophobic coatings; hydrophilic coatings; protein resistance; cell/bacteria adhesion

Citation: Choi, Y.; Tran, H.-V.; Lee, T.R. Self-Assembled Monolayer Coatings on Gold and Silica Surfaces for Antifouling Applications: A Review. *Coatings* **2022**, *12*, 1462. https://doi.org/10.3390/coatings12101462

Academic Editor: Robert J. K. Wood

Received: 11 July 2022
Accepted: 6 September 2022
Published: 4 October 2022

1. Introduction

Fouling is the accumulation of unexpected materials on a variety of surfaces [1] such as heat exchangers [2], ship hulls [3], piping [4], membranes [5], biosensors [6], and medical devices [7]. In particular, biofouling, which ranges from microorganisms to macroorganisms, diminishes the original performance of surfaces, and biofilms have adverse economic impacts on marine and medical industries [1]. For example, when boats sail in water, marine organisms are deposited on the hull surfaces due to surface friction drag, and the fouling layer later increases the surface roughness, which increases gas consumption and engine stress [8]. A low degree of biofouling increases the required shaft power by 11%, while heavy calcareous fouling has been attributed to powering penalties as high as 86%, leading to an increase of 20% in fuel consumption [9]. Moreover, surface contaminations by living organisms, including bacteria, fungi, and viruses, in a biological medium provides biofouling, resulting in a risk of infection and decreasing biosensor efficiency [10]. According to the Centers for Disease Control and Prevention, in 2011, device-associated infections in U.S. acute care hospitals accounted for 26% of healthcare-related infections [11]. Biosensors, as molecular detection devices, must operate with a minimum sample amount and contact with unrefined biomaterials, such as blood or serum. The biofluids include a variety of biocomponents in which each component undergoes nonspecific adsorption on the sensor surface, leading to severe problems with the reliability and sensitivity of results [12].

The formation of biofouling involves a multistep process. First, organic molecules, including proteins, polysaccharides and proteoglycans, and inorganic compounds are attached to the surface, forming conditioning films. The biofilm subsequently accumulates as bacteria and diatoms adhere to the surface. The attachment occurs reversibly for a short time (less than 1 min) in which the microorganisms utilize hydrodynamics (e.g., Brownian

motion, gravitation and diffusion, and physicochemical interactions such as van der Waals and electrostatic forces) to interact with the surface [13]. Furthermore, irreversible adhesion (a few hours) occurs via covalent bonding, and a biofilm is formed. Finally, this biofilm stimulates the settlement of algae and spores, followed by the attachment of macrofouling in the case of marine environments [14]. The development of biofouling formation in medical applications is similar to the processes in marine environments. When a medical device is exposed to biological media, the initial process involves nonspecific protein adsorption to the surface via hydrophobic interactions. The initial adsorption is reversible, but the protein immediately denatures and exposes more hydrophobic components, leading to irreversible attachment [15,16] and the adhesion of multiple proteins or other biomolecules (e.g., bacteria) to the protein layer.

Antifouling is a process that prevents a surface from accumulating biomolecules. Based on a mechanism of biofouling formation, the desired approach for blocking the fouling process is coating or grafting surfaces to resist the creation of biofilms that are initiated by proteins and microbes [17]. Since the discovery of tin-based compounds in the late 20th century, these compounds have been widely developed to generate antifouling coatings for ships [18]. However, since there is substantial evidence that tributyltin contamination has an adverse impact on marine organisms (e.g., the deformation of oyster shells), it is necessary to develop more biocompatible nonfouling strategies [19]. During the past decade, various antifouling strategies have been developed to prevent biofouling, and the modification of surfaces is important for minimizing biological responses [1,10,20–22]. Self-assembled monolayers (SAMs) have attracted attention for their applicability in surface tailoring methods. The SAM technique, which involves the spontaneous formation of ordered monolayer films on a surface, provides a powerful tool for tuning surface properties, such as wettability [23,24]. The procedure is straightforward, and a well-organized surface is obtained, which has a variety of applications, including surface wetting [25], adhesion [26], corrosion [27], electronic devices [28], and sensors [29]. Although several types of antifouling surfaces have been developed for use on various substrates, the majority have focused on gold or silica [1,12,20,30]. As a surface modification method, SAMs offer several attractive features for antifouling applications over other techniques. First, the easy preparation and fabrication of chemical compositions on the surface are accessible for a variety of antifouling applications, including medical equipment, biosensors, and marine environments [20,31,32]. Second, the long-term durability of the monolayer, which is created by chemisorption between headgroups and substrates, makes it possible to utilize the devices in environments such as biological media. Moreover, *N*-heterocyclic carbene (NHC)-based SAMs have recently exhibited high thermal, hydrolytic, chemical, oxidative, and electrochemical stabilities, increasing their potential applicability for biosensing applications [33,34]. Third, mixed SAMs are useful tools that either resist the nonspecific adsorption of proteins or promote the specific adsorption of proteins in the development of biocompatible sensors [30]. Last, SAMs are well-defined and well-studied and are directly feasible with a variety of techniques to analyze the thermodynamics and kinetics of binding events [35,36].

A number of analytical techniques have been widely used to study adsorption events on SAMs, such as surface plasmon resonance (SPR) spectroscopy [35–37], quartz crystal microbalance (QCM) [35,36,38], and ellipsometry [35,36,39]. Surface plasmon resonance is an optical technique that measures the changes in the index of refraction at the surface of metal layers. This instrument enables either kinetic or thermodynamic information to be acquired between artificial surfaces in a biological manner and in situ data to be collected in real time with label-free analytes; in addition, the instrument is sensitive and commercially available [20]. QCM uses the piezoelectric effect to detect the vibration frequency of quartz crystals as protein adsorbs to the surface [40]. For the QCM experiments, the choice of surface material is flexible and special precautions, such as optical reflectivity and tailored substrate compositions, are unnecessary [41]. Ellipsometry is based on the change in polarized light from the surface and the reflected light provides information about the

amount of the adsorbed protein [42]. One of the main advantages is that ellipsometry does not involve any labeling of materials and is also relatively inexpensive to maintain [43].

In this review, we describe a wide range of structural designs that are used for non-fouling SAMs and the corresponding mechanism to clarify the interactions between films and biomaterials. As outlined in Figure 1, the effects of the thin film surface, which is hydrophobic and hydrophilic, on fouling adsorption as well as the surface, which has an amphiphilic structure, are discussed. The study described in this review should inspire researchers to understand and develop novel approaches for antifouling coatings in the future. Key representative studies on the antifouling SAMs covered in this review are summarized in Table 1.

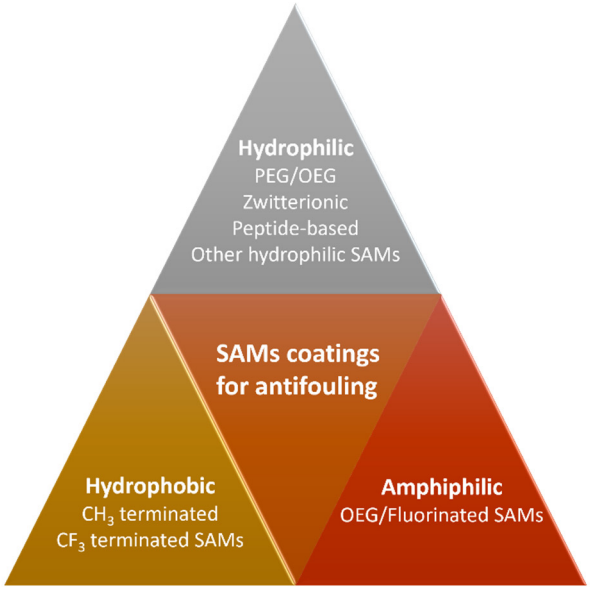

Figure 1. An overview of SAM coatings for antifouling. PEG: poly(ethylene glycol); OEG: oligo(ethylene glycol).

Table 1. Key self-assembled monolayers for antifouling applications.

Antifouling Approach	Material Type	Headgroup/Substrate	Functional Group	Detection Method	Tested Fouling Materials	Ref.
Hydrophilic	OEG	SH/Au	$-(OCH_2CH_2)_3OH$	SPR, microscope	Fibrinogen, lysozyme, *S. aureus*, *S. epidermidis*, BCE cells	[44]
		SH/Au	$-C(O)NH(CH_2CH_2O)_6CH_3$	SPR	Fibrinogen, ribonuclease A, lysozyme, carbonic anhydrase	[45]
		SH/Au	$-(OCH_2CH_2)_6OH$	Ellipsometry	RNase A, pyruvate kinase, fibrinogen	[46]
		SH/Au or Ag	$-(OCH_2CH_2)_3OCH_3$	FT-IR	Albumin, IgG, fibrinogen	[47]
		SH/Au	$-(OCH_2CH_2)_nOH$ n = 2, 4 and 6	SPR	Fibrinogen, lysozyme, BSA	[48]
		SH/Au	$-(OCH_2CH_2)_6OR$ R = H or CH_3	Ellipsometry	Fibrinogen, pyruvate kinase, lysozyme, ribonuclease A	[49]
		SH/Au	$-(OCH_2CH_2)_nOR$ n = 1, 2, 3, 6 and R = H, CH_3, CH_2CH_3, $CH_2CH_2CH_3$	Ellipsometry	Fibrinogen	[50]

Table 1. *Cont.*

Antifouling Approach	Material Type	Headgroup/Substrate	Functional Group	Detection Method	Tested Fouling Materials	Ref.
		SH/Au	$-(OCH_2CH_2)_3OH$	SPR	BSA, *β*-galactosidase, carbonic anhydrase II, fibrinogen, myoglobin, ribonuclease A, cytochrome *c*, lysozyme	[51]
		SH/Au	$-(OCH_2CH_2)_3OH$	Microscope	*S. epidermidis*, *P. aeruginosa*, 3T3 fibroblasts	[52]
		SH/Au	$-(OCH_2CH_2)_3OH$	SPR, microscope	Fibrinogen, pepsin, lysozyme, insulin, trypsin 3T3 fibroblast	[53]
		SH/Au	$-C(O)NH(CH_2CH_2O)_nR$ n = 3, 6 and R = H, CH_3	SPR	Fibrinogen, lysozyme	[54]
	Zwitterion	SH/Au	$-OP(O)_2{}^-OCH_2CH_2N^+(CH_3)_3$ $-N^+(CH_3)_2CH_2CH_2CH_2SO_3{}^-$	SPR, microscope	Fibrinogen, lysozyme, *S. aureus*, *S. epidermidis*, BCE cells	[44]
		SH/Au	$-OP(O)_2{}^-OCH_2CH_2N^+(CH_3)_3$	QCM	BSA, fibrinogen, FBS	[38]
		SH/Au	1:1 mixture of $-OPO_3{}^-$ and $-N^+(CH_3)_3$	SPR	Fibrinogen	[55]
		SH/Au	$-SO^{3-}$ $-N^+(CH_3)_3$ $-N^+(CH_3)_2CH_2CH_2CH_2SO_3{}^-$ $-OP(O)_2{}^-OCH_2CH_2N^+(CH_3)_3$	SPR	BSA, *β*-galactosidase, carbonic anhydrase II, fibrinogen, myoglobin, ribonuclease A, cytochrome *c*, lysozyme	[51]
		SH/Au	$-OP(O)_2{}^-OCH_2CH_2N^+(CH_3)_3$	SPR	Fibrinogen, BSA	[56]
		SH/Au	$-CH(N^+(CH_3)_3)COO^-$	Microscope	*S. aureus*, *S. epidermidis*, 3T3 fibroblasts	[52]
		SH/Au	$-CH(N^+(CH_3)_3)COO^-$	ELISA, microscope	BSA, lysozyme, mucin, *S. aureus*, *S. epidermidis*, 3T3 fibroblasts	[57]
	Peptide-base	SH/Au	Magainin I	Microscope, AFM, PM-IRRAS	*L. ivanovii*, *E. faecalis*, *S. aureus*	[58]
		SH/Au	Glutamic acid/lysine peptide	SPR	Fibrinogen, lysozyme	[59]
	Others	SH/Au	Permethylated sorbitol	SPR, microscope	Fibrinogen, lysozyme, *S. aureus*, *S. epidermidis*, BCE cells	[44]
		SH/Au	Saccharide	Ellipsometry, microscope	Lysozyme, fibrinogen, BSA, pepsin, *Ulva linza*, *Balanus amphitrite*	[60]
		SH/Au	Mannitol	SPR, microscope	Fibrinogen, pepsin, lysozyme, insulin, trypsin 3T3 fibroblast	[53]
		SH/Au	Dendritic polyglycerol	SPR	Fibrinogen	[61]
		SH/Au	Saccharide or sorbitol	SPR	Fibrinogen, lysozyme	[54]

Table 1. *Cont.*

Antifouling Approach	Material Type	Headgroup/Substrate	Functional Group	Detection Method	Tested Fouling Materials	Ref.
Hydrophobic	-	Silane/SiO_2	$-(CF_2)_7CF_3$	Microscope	*Ulva linza*	[62]
		SH/Au	$-(CH_2)_{11}CH_3$	Microscope	*N. europaea*, *N. multiformis*, *E. coli*	[63]
		Silane/SiO_2	$-(CF_2)_7CF_3$ $-(CH_2)_7CH_3$	SDS-PAGE and immunoblotting, bicinchoninic acid assay	Human saliva, serum	[64]
		Silane/SiO_2	$-(CF_2)_5CF_3$	Microscope	Fibroblast cells, embryonic stem cells	[65]
		SH/Au	$-(CH_2)_{11}CH_3$	SPR, microscope	*C. marina*, *M. hydrocarbonoclasticus*	[66]
		Silane/SiO_2	$-(CH_2)_{17}CH_3$	Microscope	Fibroblasts	[67]
		Silane/SiO_2	$-(CH_2)_{17}CH_3$ $-(CF_2)_5CF_3$	Microscope	Astrocyte, Choroid plexus,	[68]
		$(CH_2SH)_2$/Au	1:1 mixture of $-(CH_2)_8(CF_2)_7CF_3$ and $-(CH_2)_{15}CH_3$	Ellipsometry, QCM, SPR	Protamine, lysozyme, BSA, fibrinogen	[35]
Amphiphilic	-	$(CH_2SH)_2$/Au	1:1 mixture of $-(CH_2)_5(OCH_2CH_2)_3OCH_3$ and $-(CH_2)_{15}CH_3$	Ellipsometry, QCM, SPR	Protamine, lysozyme, BSA, fibrinogen	[25,36]
		SH/Au	1:1 mixture of $-(OCH_2CH_2)_3OH$ and $-(CF_2)_7CF_3$	SPR, microscope	BSA, fibrinogen, immunoglobulin, Hela cell	[69]

Abbreviations: BCE: bovine capillary endothelial; IgG: immunoglobulin G; FT-IR: Fourier transform infrared spectroscopy; BSA: bovine serum albumin; FBS: fetal bovine serum; ELISA: enzyme-linked immunosorbent assay; AFM: atomic force microscopy; PM-IRRAS: polarization modulation infrared reflection–absorption spectroscopy; OEG: oligo (ethylene glycol); SPR: surface plasmon resonance; QCM: quartz crystal microbalance.

2. Hydrophilic Antifouling SAMs

Remarkable progress has been made in self-assembled monolayers for antifouling since Prime et al. pioneered the study of protein adsorption with SAMs on gold [46]. They demonstrated that the amount of protein adsorbed varied with the monolayers that contained different terminal groups of adsorbates on the gold surface. This study demonstrated that SAMs provide various surface properties depending on the molecules on the substrate that are hydrophilic or hydrophobic; thus, SAMs are an effective system for examining the relationship of proteins and surfaces regarding the mechanisms of these interactions. The most common SAM system that has been studied for anti-adhesive coatings involves increasing the surface hydrophilicity, which generates hydration layers as a surface barrier [47,48]. The adsorbates for applying hydrophilic functionalization include adsorbates with polyethylene glycol (PEG) [70], oligo (ethylene glycol) (OEG) [47–50,71], zwitterion [38,51,52,55–57], peptide [58,59] and other hydrophilic materials, such as mannitol [53], saccharide [60] and polyglycerol [61].

2.1. PEG and OEG SAMs

PEG chains have been commonly used for antifouling coatings due to their biocompatibility, nonimmunogenicity, nonantigenicity, and nontoxicity [72]. Although the detailed mechanism of prevention is not fully understood, the most acceptable explanation of the resistance to proteins by PEG is the steric repulsion between highly hydrated PEG and biomolecules [73]. Once PEG is fully hydrated by water, the mobility or flexibility of the immobilized chain on the surface increases. When biomaterials approach the hydrated PEG layer, the biomaterials compress the PEG chains and then the repulsive elastic force of PEG, which generates a higher entropy, prevents adsorption to the surface. Thus, the entropy-driven steric effect is attributed to the antifouling mechanism of biomolecules from PEG-coated surfaces.

While PEG-based adsorbates have been widely used for antiadhesive coatings since the early 1980s, OEG-based SAMs are useful as a nonfouling coating model to elucidate the relationships between the surface and the adsorption of biomaterials because they are easy to prepare and their topology can be controlled by varying the terminal group during the synthesis of the precursor, which is nearly constant from sample to sample [49]. However, unlike surface coatings with polymers, SAMs exhibit a high density of molecules on the surface, and the antifouling property cannot be explained only via the steric repulsion theory, as applied in the PEG coating [55]. When the protein approaches densely packed SAMs that contain only a few ethylene oxide groups, it is clear that the steric repulsion is lower than that of the PEG surfaces because the conformational freedom of the chain is strained (Figure 2, left).

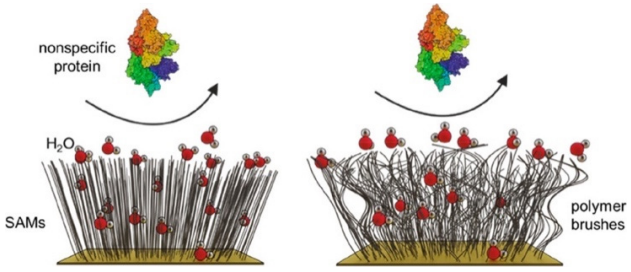

Figure 2. Hydration of highly packed OEG (3–10 ethylene glycol units) SAMs (**left**) and flexible PEG (>10 ethylene glycol units) polymer (**right**), which are implicit in protein resistance [30]. Copyright 2020 American Chemical Society.

Instead, the interfacial water that strongly binds to the molecule plays a critical role in the resistance to biomaterials. The polar groups on the surface form a hydration layer via hydrogen bonding. Adsorbing biomolecules to this surface simply involves the disconnection of hydrogen bonds between water and the surface followed by replacement with the functional groups of biomaterials; this process is not thermodynamically favorable [74]. From this point of view, researchers have focused more on the importance of the water layer in hydrophilic SAMs and their resistance to protein adsorption. Whiteside et al. reported a study of the adsorption of four proteins to SAMs on gold [49]. In this pioneering work, SAMs derived from thiols of $HS(CH_2)_{10}CH_3$ and $HS(CH_2)_{11}(OCH_2CH_2)_nOR$, in which n = 0–17 and R = H or CH_3, were tested to investigate the effects of the length and number of ethylene oxide (EG) groups on protein resistance. The data showed that relatively densely packed SAMs with a few EG units (at least two EG units) effectively resist protein adsorption and concluded that the steric repulsion theory does not critically contribute when attempting to fully understand protein resistance. This observation clearly demonstrated that SAMs could cover a large number of chains per unit surface area with shorter chain lengths than those of other techniques for antifouling purposes.

Moreover, subsequent studies demonstrated that the protein resistance of OEG SAMs is attributed to their molecular conformation, which provides a repulsive hydration layer between the solvated hydrophilic chain and the biomaterials [47,50,71,75]. Feldman et al. investigated the electrostatic repulsive forces that act toward EG3OMe SAMs with a protein immobilized AFM probe in buffer solutions [71]. They demonstrated that electrostatic repulsion was generated toward the film of EG3OMe on gold when the fibrinogen attached AFM tip was approaching, while no electrostatic repulsion occurred with the film on Ag; instead, there was strong adhesion between the film and protein. Harder et al. supported the idea that the repulsive force between protein and OEG-based alkanethiol SAMs on gold or silver contributes to the molecular conformation of OEG moieties [47]. FTIR spectra demonstrated that the methoxy-terminalized OEG (3 EG units) films have helical and amorphous structures on gold, which was found to have a higher fibrinogen resistance, while the OEG film on silver contains all-trans conformations and adsorbs fibrinogen. The conformation of the OEG-terminated alkanethiol film can be explained by the lateral

spacing of the alkane chains. Due to the tilt of the alkane chains, the OEG forms a helical conformation on gold, while the alkane chains are almost perpendicular to the surface, and the OEG units have trans conformations as a consequence (Figure 3).

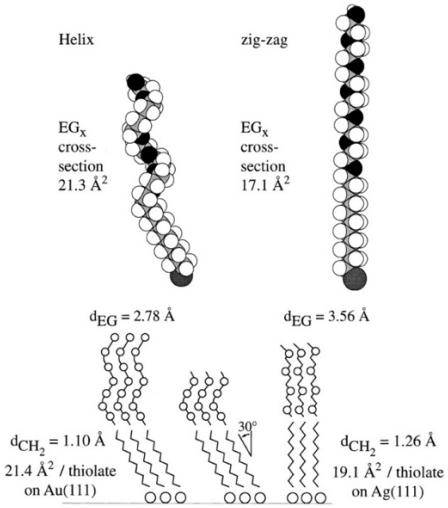

Figure 3. EG6-OH and EG3-OMe with a 30° tilt of the alkyl chain with a helix of EG units on gold and a zigzag conformation of EG units on Ag [47]. Copyright 1998 American Chemical Society.

The researchers assumed that the conformation of OEG consequently affects the stability of an interfacial water layer and protein adsorption. Moreover, Herrwerth et al. clearly demonstrated that the combination of terminal and internal hydrophilicity and the lateral packing density are the key factors in determining protein resistance [50]. Oligo(ethylene glycol), oligo(propylene glycol), and oligo(trimethylene glycol)-terminated alkanethiols with different chain lengths were tested as adsorbates. The packing density, surface hydrophilicity, and chain conformation of the SAMs were examined by XPS, contact angle, and infrared reflection absorption spectroscopy (IRRAS), respectively. The results showed that: (1) hydrophobic units, such as oligo(propylene glycol), barely affect protein resistance, highlighting the importance that the SAMS are accessible to water; (2) the lateral high packing of oligo(ethylene glycol) SAMs on silver contributes to low protein resistance; and (3) water contact angles greater than 70° reduce protein resistance. Similar to experimental efforts, molecular simulation data have also supported the importance of the hydration layer [75,76]. The grand canonical Monte Carlo simulation results demonstrated that water penetrates well through the helical SAM of EG3OMe on gold due to its lower areal density, leading to the formation of water layers with a large number of water molecules at the surface, while water can barely penetrate the conformationally ordered films on silver, enhancing protein adsorption.

2.2. Zwitterionic SAMs

Zwitterionic materials are materials that have both cationic and anionic moieties on the same monomer unit [77]. Since zwitterionic materials can bind water molecules tightly via strong electrostatic interactions, while hydrophilic PEG/OEG molecules form hydration via hydrogen bonds on the surface, it is expected that zwitterionic materials with strong ionic solvation can be potential candidates for nonfouling applications [78,79]. Moreover, due to their antifouling properties and biocompatibility [80], zwitterionic materials are a new class of protein resistance materials [51,56,57]. Holmlin et al. demonstrated the ability of SAMs that contain zwitterionic groups in different combinations to resist the adsorption of proteins [51]. In their studies, the researchers provided different kinds of adsorbates deposited on gold and utilized fibrinogen and lysozyme adsorption with each SAM as follows: (1) single-charged SAMs (all positive or all negative as shown in Figure 4C,D) exhibited no resistance of adsorption to proteins, (2) the films generated from

a 1:1 mixture of negatively and positively terminated thiols (Figure 4E) clearly exhibited resistance to nonspecific protein adsorption, which is comparable to the data from OEG-based SAMs, and (3) single-component SAMs formed from thiols possessing both positive and negative charges in one molecule (Figure 4F) enabled good resistance to the adsorption of proteins (Figure 4).

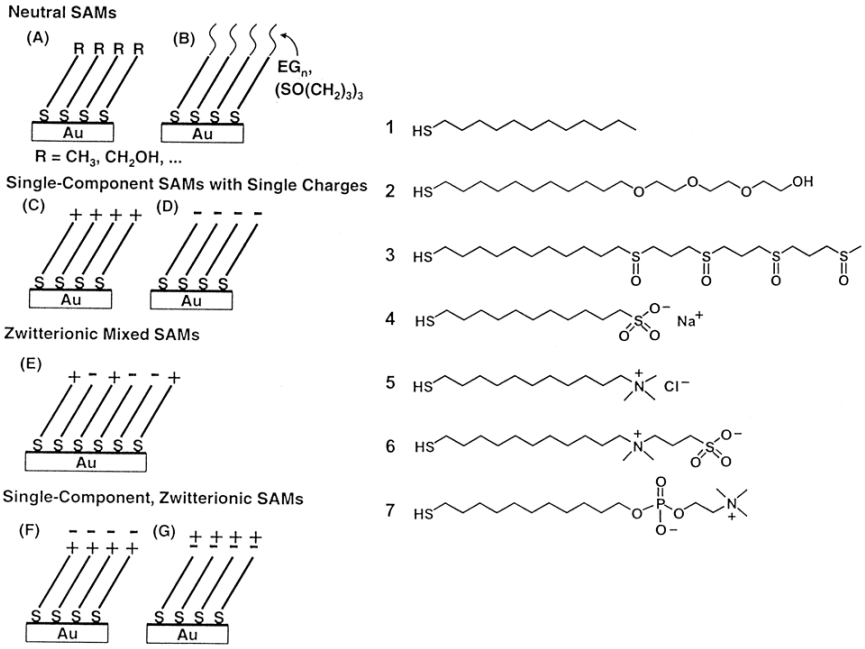

Figure 4. Illustrations of SAMs formed from different combinations of charged molecules and detailed structures of the adsorbates used in this study [51]. Copyright 2001 American Chemical Society.

These results demonstrated that one of the prerequisites for zwitterionic SAMs to exhibit protein resistance is electrical neutrality. Jiang et al. also reported the strong resistance of phosphorylcholine (PC) SAMs to protein adsorption using both experimental and molecular simulation techniques [56]. The generated zwitterionic PC SAMs were evaluated with the adsorption of fibrinogen and BSA. PC SAMs are highly resistant to proteins according to the SPR data; the amount of adsorption to the surface was 0.03 mg/m^2 and 0.01 mg/m^2 for fibrinogen and BSA, respectively. The researchers stated that the key factors resulting in a strong resistance of zwitterionic SAMs included minimized dipole interactions and balanced charges. Based on the XPS spectra, the PC SAMs had negative and positive charges at a 1:1 ratio and these SAMs exhibited a higher antifouling with fibrinogen compared to that of the SAMs at a ratio of 0.87:1. Furthermore, the molecular simulation results showed that the orientation of the PC headgroups is parallel to the gold surface and that the headgroups favor an antiparallel orientation to each other to minimize the net dipole moment, as shown in Figure 5.

This conformation was supported by the experimental data. The thicknesses of the PC SAMs were measured by ellipsometry and AFM and were 9 Å and 14 Å, respectively, which is significantly lower than the expected thickness of PC SAMs (21 Å). Therefore, it is expected that the orientation of the PC headgroups lies perpendicular to the surface normal. In 2015, Huang et al. developed an L-cysteine-derived zwitterionic molecule (L-cysteine betaine) and investigated the antifouling properties of the corresponding SAMs [57]. In contrast to L-cysteine (Cys), L-cysteine betaine (Cys-b) has a durable zwitterionic form from pH 3.4 to 10.8 and the quaternization of the amine group efficiently reduces photoinitiated oxidization (Figure 6). The researchers conducted fouling resistance tests with SAMs from Cys and Cys-b on gold in bacteria, proteins, and mammalian cells. For the bacterial resistance test, the film generated from Cyc-b showed higher antifouling properties even after photooxidation, while Cys SAMs adsorbed a higher number of bacteria (Figure 6, left).

Moreover, the results demonstrated the greater ability of the Cys-b-coated surfaces to resist the adsorption of mucin, lysozyme, and BSA compared to the Cys SAMs (Figure 6, middle). The study of the adhesion of mammalian cells also indicated that NIH 3T3 cells adsorbed more on Cys-based SAMs than on Cys-b SAMs (Figure 6, right). The higher antifouling system of Cys-b SAMs can be rationalized by the fact that the association of quaternary ammonium and carboxylate groups is attributed to strong hydration, low self-association of ionic groups, and low electrostatic attraction to proteins according to the molecular simulation study [81].

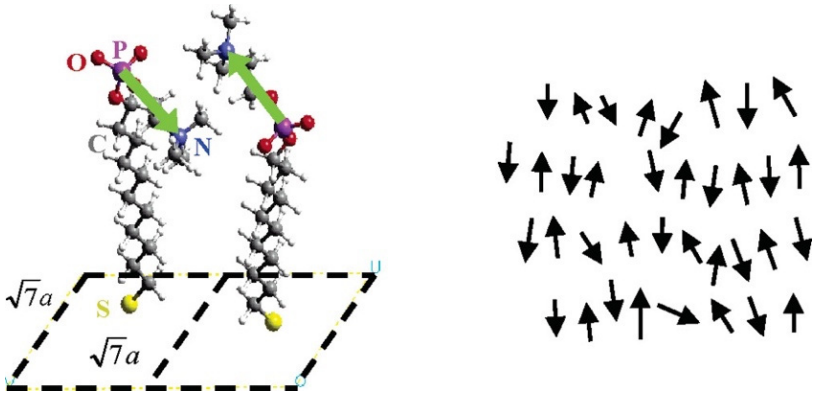

Figure 5. Molecular configuration of phosphorylcholine SAMs (**left**) and antiparallel orientation of the headgroups (**right**) [56]. Copyright 2005 American Chemical Society.

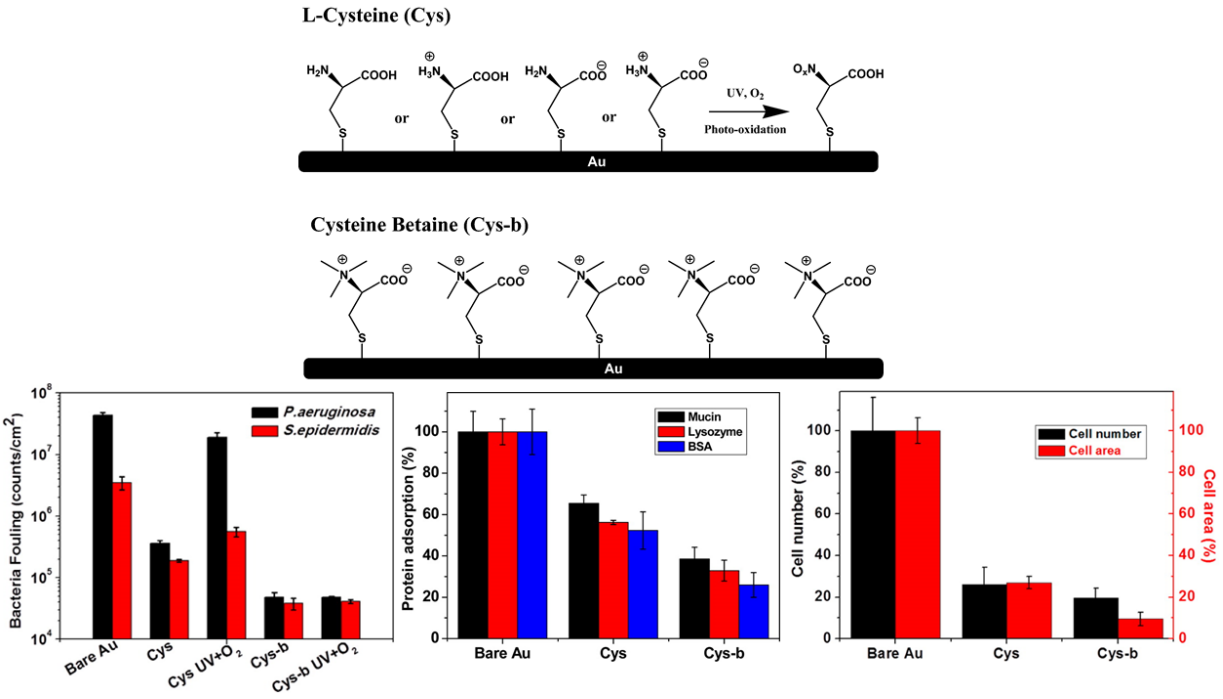

Figure 6. Zwitterionic adsorbate structure and fabrication on the gold used in this study. The quantitative results for bacterial adsorption (**left**), protein adsorption (**middle**), and relative cell adsorbed number and cell spreading area (**right**) [57]. Copyright 2015 American Chemical Society.

2.3. Peptide-Based SAMs

Given that peptides are biocompatible and can exhibit a variety of characteristics, including hydrophilicity, charge, conformational rigidity, anchoring ability, and facile functionalization with specific sequences, peptide-based SAMs represent a promising class of antifouling coatings [82]. Several approaches have recently been studied for this pur-

pose, including the use of antimicrobial peptide agents [58] and zwitterionic peptides [59]. Humblot et al. reported a study of the antibacterial surface of peptide Magainin I [58]. Antimicrobial peptides, which are produced by plants, insects, mammals, and microorganisms, provide a wide spectrum of activity against bacteria and other pathogens at low concentrations. In these studies, Magainin I, an antimicrobial peptide, was immobilized on a gold surface by co-adsorption with a binary mixture of thiol 11-mercaptoundecanoic acid and 6-mercaptohexanol followed by a coupling reaction with *N*-hydroxysuccinimide in the presence of a carbodiimide reagent (Scheme 1).

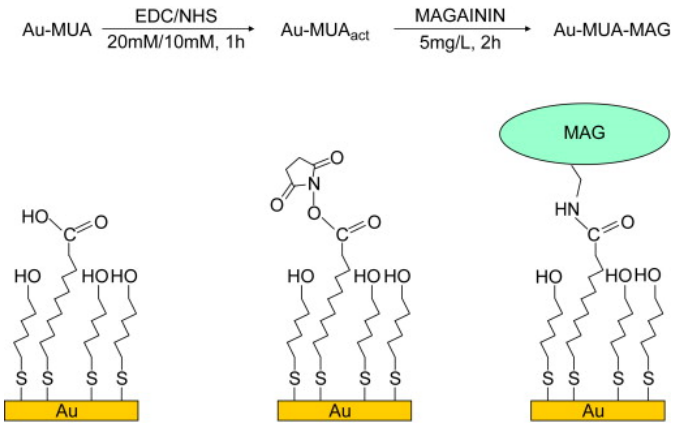

Scheme 1. Magainin I immobilization on gold [58]. MUA: 11-mercaptoundecanoic acid; EDC: 1-(3-dimethylaminopropyl)-*N′*-ethyl-carbodiimide hydrochloride; NHS: *N*-hydroxysuccinimide. Copyright 2009 Elsevier Ltd.

Three gram-positive bacteria (*L. ivanovii*, *E. faecalis*, and *S. aureus*) were deposited on Au-MUA-MAG (Magainin I modified film) or Au-MUA (without Magainin I) at 37 °C for 3 h. The surface modified with Magainin I (Au-MUA-MAG) effectively inhibited the adhesion of each gram-positive bacterium, preventing 80% of *L. ivanovii* cell attachment compared to that of the untreated surface (Au-MUA). Moreover, the antibacterial activity of the Margainin-functionalized surfaces persisted even after 6 months. The researchers suggested that Magainin induced the formation of pores in the lipids of targeted cell membranes, leading to microorganism cell lysis and they confirmed the observation that the adhered bacterial cell surface deteriorated with the collapse of cell walls. Zwitterionic peptides can provide another way to prevent biofouling, as water molecules are strongly bound via electrostatic interactions with peptide residues [77]. Nowinski et al. reported an ultralow fouling monolayer on a gold surface with alternating negatively charged glutamic acid (E) and positively charged lysine (K) residues [59]. The structure of SAMs in this study was composed of (1) a cysteine (C) residue as an anchor to bind gold, (2) four proline (P) linker residues, which provide hydrophobicity and helical secondary structure, (3) an alternating glutamic acid (E) and lysine (K) sequence to form a strong hydration layer and (4) an arginine–glycine–aspartate (RGD) sequence mimicking extracellular matrix proteins as a biomolecular recognition (Figure 7). To compare the impact of rigid and hydrophobic proline linker (EKEKEKE-PPPPC), the researchers used the flexible and hydrophilic glycine residue as a linker (EKEKEKE-GGGGC) as well as the linker-free peptide (EKEKEKE-C). SPR data show that the fouling of fibrinogen to the EKEKEKE-PPPPC SAMs is 4.4 ± 2.9 ng/cm^2, while it is 17.9 ± 11.4 ng/cm^2 for the EKEKEKE-GGGGC SAMs and 38.3 ± 2.9 ng/cm^2 for the EKEKEKE-C SAMs. To study the different amounts of fouling in greater depth, the researchers examined the secondary structure of each peptide in solution using circular dichroism (CD), molecular dynamics (MD) simulations, and attenuated total internal reflection Fourier transform IR spectroscopy (ATR-FTIR). The CD, MD, and ATR-FTIR data supported that the proline linker contained an extended and rigid helical structure, allowing peptide chains to pack well with each other, while the linker-free

(EKEKEKEKE-C) and glycine linker (EKEKEKEKE-GGGGC) peptides exhibited disordered structures, compromising their antifouling properties.

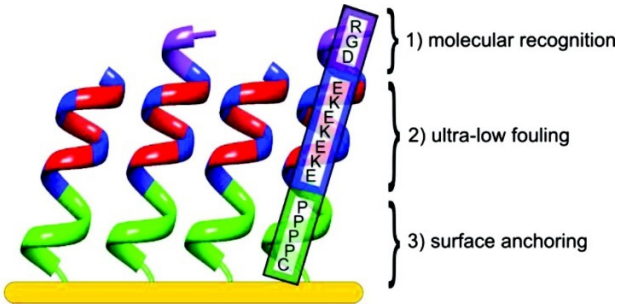

Figure 7. Three different sequences incorporated in natural peptide SAMs on gold [59]. Copyright 2012 American Chemical Society.

2.4. Other Hydrophilic SAMs

In 2001, Ostuni et al. investigated SAMs that contain different functional groups and their protein resistance via SPR [54]. In these studies, the functional groups, which showed acceptable results for the prevention of protein adsorption, exhibited the following molecular-level characteristics: (1) the group is hydrophilic, (2) the group includes hydrogen bond acceptors but does not have hydrogen bond donors, and (3) the overall electrical charge is neutral. In particular, the researchers used multiple amine functional groups, such as glycine and sarcosine, and replaced one of the hydrogen atoms on the amino group with a methyl group to test the effect of hydrogen donors on protein resistance; the substitution reduced protein adsorption to the surface. However, a molecular exception to these general requirements was reported [53,61]. Specifically, in 2000, Luk et al. reported that mannitol-terminated SAMs are remarkably effective for producing inert surfaces against protein adsorption and cell adhesion [53]. The authors generated films possessing terminal mannitol groups (Figure 8, surface 2) that were comparable to OEG monolayers (Figure 8, surface 1) in repelling five proteins, including fibrinogen pepsin, lysozyme, insulin, and trypsin. Moreover, the mannitol SAMs maintained good anti-adherent of cells over 25 days, while the OEG SAMs failed after 7 days. Molecular simulation results suggest that mannitol SAMs are tightly bound with water and that the hydration layer generated a strong repulsive force on the approaching proteins despite the presence of hydrogen bond donor groups [83]. Along with the mannitol group, Siegers et al. also studied the nonspecific protein adsorption of dendritic polyglycerol SAMs, which contain several hydrogen bond donors [61]. The dendritic polyglycerol SAMs exhibited an effective inertness to fibrinogen adsorption compared to that of the OEG SAMs and showed more protein resistance than that of a commercially available dextran-based sensor chip. In addition to their antifouling ability, dendritic polyglycerols also exhibited higher thermal and oxidative stability than PEG. Dendritic polyglycerols contain the following structural features that are typical of protein-resistant surfaces: (1) hydrophilic repeating units, which are water-soluble, and (2) a very flexible branched structure, which leads to high protein resistance (Figure 8). Excellent resistance against protein absorption was observed with those features, even though molecules with hydrogen bond donor OH groups were opposed to the general rule for the inert surfaces.

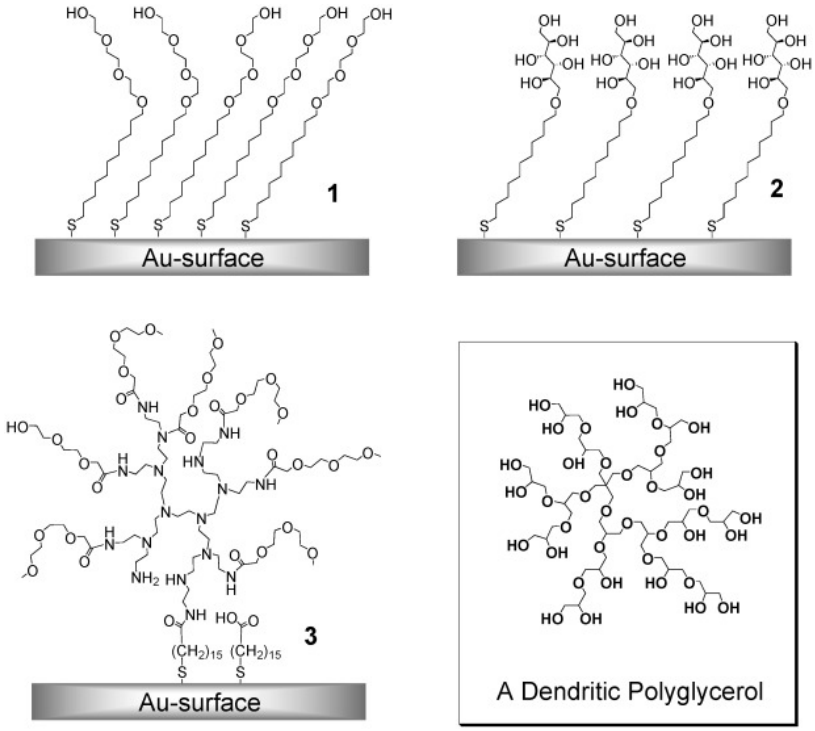

Figure 8. Highly protein-resistant surfaces (**1**–**3**): SAMs presenting oligo(ethylene glycol) groups (**1**), SAMs involving mannitol groups (**2**), SAMs with a highly branched architecture (**3**), and a dendritic polyglycerol group for antifouling SAMs [61]. Copyright 2004 WILEY-VCH Verlag GmbH & Co. KGaA, Weinheim.

3. Hydrophobic Antifouling SAMs

There are two general strategies by which surface modification inhibits biomaterial adsorption: (1) prevention of biomaterial attachment and (2) detachment of biofoulants [84]. In the strategy involving the prevention of biomaterial attachment, settlement of biomolecules on the surfaces is avoided such as using a strong hydration barrier as we discussed above. On the other hand, the strategy involving the detachment of biofoulants provides only a weak connection between the surface (mainly the hydrophobic surfaces) and the biomaterials. Thus, the goal of the strategy is to reduce adhesion by removing the settled organisms from the surface using stresses such as the hydrodynamic flow caused by ship movements. Removing marine organisms from hydrophobic surfaces has a strong relationship with the low surface energy of materials. The correlation between the relative adhesion of biomaterials and the surface energy of the polymer was reported by Baier [85]. The Baier curve has been used to depict the degree of biofouling adhesion as a function of the critical surface tension (Figure 9).

Critical surface tension corresponds to the surface tension of a liquid that perfectly wets the solid surface, as introduced by Zisman [86]. Baier's empirical study stated that the material's critical surface tension must be between 20 and 30 mN/m, which is efficient in preventing the adhesion of marine biofoulants. A possible explanation was provided by Scharader based on the Good–Girifalco–Fowkes theory [87]. He explained that the excess dispersion forces stem from the solid surface in the high critical surface tension range (above 22 mN/m) and the forces also originate from the liquid surface in the low critical surface tension range (below 22 mN/m). Thus, both excess dispersion forces of the solid and liquid result in an increase in the total interaction at the interface. When the critical surface tension is equal to 22 mN/m, which is the same as the dispersive component of the surface tension of water, the dispersion force is zero and the total interfacial force is minimal. The surfaces with low critical surface energy values are typically closely packed with methylated materials and polyvinylidene fluoride (PVDF). The low surface energies

on those polymers emanate from the exposed CH_3 and CF_3 moieties at the interfaces. The surface energy of hydrophobic moieties decreases in the following order: $-CH_2$ (36 mN/m) > $-CH_3$ (30 mN/m) > $-CF_2$ (23 mN/m) > $-CF_3$ (15 mN/m) [84]. Thus, closely packed alkyl or perfluoroalkyl groups on surfaces minimize the surface energies, reducing molecular diffusion and rearrangement when exposed to biomolecules.

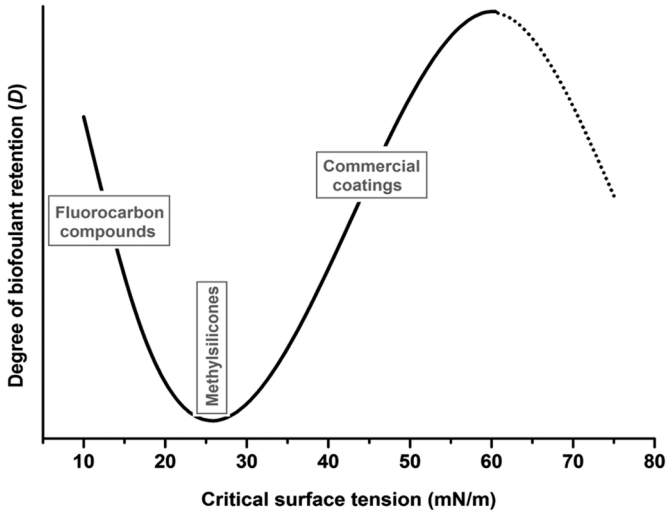

Figure 9. The relative amount of biofouling versus the critical versus tension of various materials [84]. Copyright 2015 The Royal Society of Chemistry.

However, research on the adsorption of biomolecules to polymer substrates has been difficult and ambiguous, especially regarding the definition of the surface and fouling interactions at the molecular level because it is difficult to limit the region of the surface interacting with biomolecules [88]. Consequently, there are increasing applications of SAMs in antifouling areas via a systematic change in surface energy, allowing reproducible results on functionalized surfaces [62–64,89]. Moreover, hydrophobic SAMs generated by alkyl- or perfluorinated chains offered an efficient way to prevent protein [64,65], bacterial [63,66], and cell [62,67,68] adhesions. In particular, BSA adsorption on perfluorooctyl-terminated SAMs is approximately 78% of that on glass substrates [65]. The amount of adsorbed saliva is as low as <20 ng/cm^2 for CH_3- and CF_3-terminated SAMs, compared to 50 ng/cm^2 for NH_2- and SO_3H-terminated SAMs [64]. For serum proteins, very small amounts of adsorbed proteins were measured for CH_3- and CF_3-based thin films and those values are similar to the adsorbed proteins on PEG SAMs [64]. Furthermore, CH_3 SAMs showed a low attachment rate against two autotrophic ammonia-oxidizing bacteria (*Nitrosomonas europaea* and *Nitrosospira multiformis*) and a heterotroph (*Escherichia coli*) [63]. 1-Hexadecanethiol SAMs and (11-mercaptoundecyl)hexa(ethylene glycol) SAMs exhibited the highest resistances to *M. hydrocarbonoclasticus* and *C. marina* adhesion among six different kinds of organo-sulfur compound-based SAMs [66]. These studies found that Ulva spores were less spread over the surfaces of hydrophobic CH_3-alkanethiol and CF_3 monolayers compared to that of hydrophilic OH-alkanethiol SAMs [62]. The attachment of fibroblast cells that adhered to CH_3-terminated SAMs was weak and similar to that of PEG and OH SAMs [67]. Following the same trend, fluoroalkylsilane SAMs significantly reduced *astrocyte* and *choroid plexus* proliferation, while hydrophilic biopolymer-coated surfaces (heparin and hyaluronan) increased cell growth [68].

Recently, St. Hill et al. reported antifouling thin films that were generated from unsymmetrical and partially fluorinated spiroalkanedithiols on gold [35]. To study protein adsorption on the interfacially conflicted monolayers, the researchers generated SAMs from mixed spiroalkanedithiols that were unsymmetrical and partially fluorinated, including F8H10-C12 and F8H10-C18, and compared them to SAMs that were generated from single component adsorbates, n-alkanethiol and partially fluorinated alkanethiol (Figure 10). The

antifouling performance was evaluated with four proteins, including protamine, lysozyme, BSA, and fibrinogen, using not only ex situ ellipsometric thickness and electrochemical QCM measurements but also in situ surface plasmon resonance spectroscopy (SPR). The SPR and QCM data indicated that protein adsorption was more resistant with the thin films with hydrocarbon/fluorocarbon mixed bidentate adsorbates on gold than with single-component SAMs. The improved resistance to protein adsorption for the two-phase incompatible hydrocarbon and fluorocarbon mixed surfaces can be rationalized by their unnatural compositions that are not found in nature.

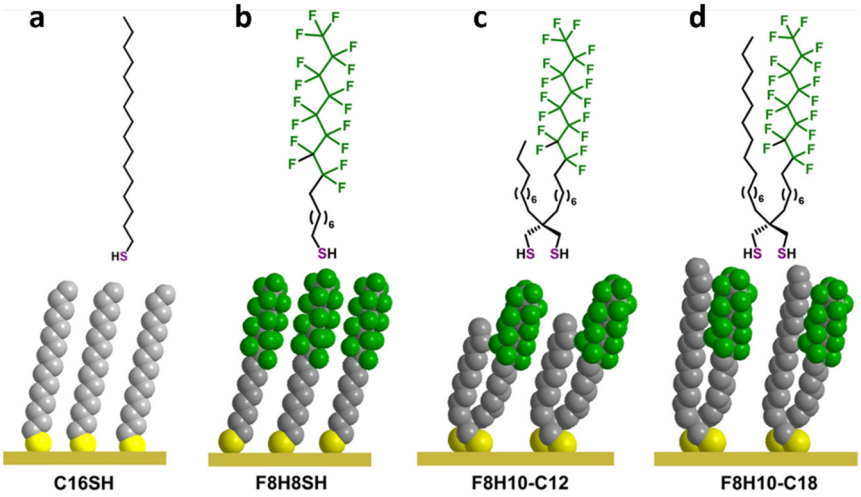

Figure 10. Adsorbate structures of the monodentate thiolates (**a**) **C16SH** and (**b**) **F8H8SH**), and unsymmetrical partially fluorinated spiroalkanedithiols (**c**) **F8H10-C12** and (**d**) **F8H10-C18**). Adapted with permission from reference [35]. Copyright 2021 American Chemical Society.

4. Amphiphilic Antifouling SAMs

Considering that hydrophilic coatings via SAMs prevent the adsorption of proteins and attachment of bacteria and marine organisms [38,47–53,55–57,59–61], and that hydrophobic SAM surfaces are able to release biomaterials [62–68] as shown through previous studies, the SAM technique is truly a useful strategy for designing effective antifouling coatings. PEG/OEG or zwitterionic molecules are among the most widely used hydrophilic materials and the surfaces generated from those compounds contain water molecules via hydrogen bonding or electrostatic force, leading to strong hydration layers and a thermodynamic advantage for biomolecule resistance. Despite their excellent antifouling performance, PEG and OEG moieties lack long-term stability and are vulnerable to oxidation [54]. Moreover, OEG SAMs showed quite extensive adsorption of proteins from blood plasma and serum [90], and zwitterionic SAMs could not reduce the attachment of *S. aureus* and *S. epidermidis* [44] even though both types of SAMs greatly reduced single-component protein adsorption. In addition, hydrophobic surfaces composed of CH_3- or CF_3-terminated monolayers readily released organisms by weakening the adhesion of foulants to surfaces due to their low surface energies, facilitating the removal of attached biomaterials. On the other hand, it is interesting that for the hydrophobic CH_3 SAMs, a very low attachment of *P. aeruginosa* was observed, while attachment of *S. epidermidis* on the hydrophobic CH_3 terminated surface was much higher than that on glass substrates [91]. In the blood incubation experiments, no leukocytes were observed on CH_3-terminated SAMs, although many strongly deformed platelets were attached to this surface [92].

Indeed, the adsorption of proteins, bacteria, and cells are affected not only by the surface properties (e.g., hydrophobic or hydrophilic), but also by the kind of biomaterials adsorbed [42,93]. For example, proteins are complex biocompounds composed of ~20 amino acids with possible additional side chains, such as phosphates, oligosaccharides, or lipids. Due to this functional complexity and diversity, it is difficult to make simple judgments to understand the adsorption process fully; lipoproteins are structurally labile and

thus have conformational reorientations, which are readily adsorbed to the hydrophobic surface, while a high content of hydrophilic glycans on glycoproteins adsorb extensively on hydrophilic surfaces and sparsely on hydrophobic surfaces [42]. Moreover, marine organisms, including shells (barnacles, mussels, and bryozoans) and soft-fouling species (tunicates, macroalgae, hydroides, slime, diatoms, and bacteria), can attach to surfaces in many forms, and the adhesives used by these organisms are equally varied [93]. Hence, such a variety of biomaterials, which are involved in the complex attachment and adhesion processes, have inspired the development of new antifouling coatings. The general idea of amphiphilic coatings is to include on one surface both nonpolar and hydrophilic moieties to reduce polar interactions with biomolecules in combination with the well-known "detachment of fouling" approach of hydrophilic groups. This chemical ambiguity or heterogeneity may lower the entropic and enthalpic driving forces for the adsorption of protein and glycoprotein organisms, which exhibit amphiphilic characteristics [94].

Recently, Chinwangso et al. developed and characterized the properties of thin films that are composed of chemically disparate species [25]. In the study, new unsymmetrical spiroalkandithiol adsorbates having within one molecule a chain possessing three EG units and another chain possessing an alkyl group. These adsorbates were designed to overcome the issue of phase separation that was generated from the co-adsorption of two separate monodentate adsorbates (Figure 11).

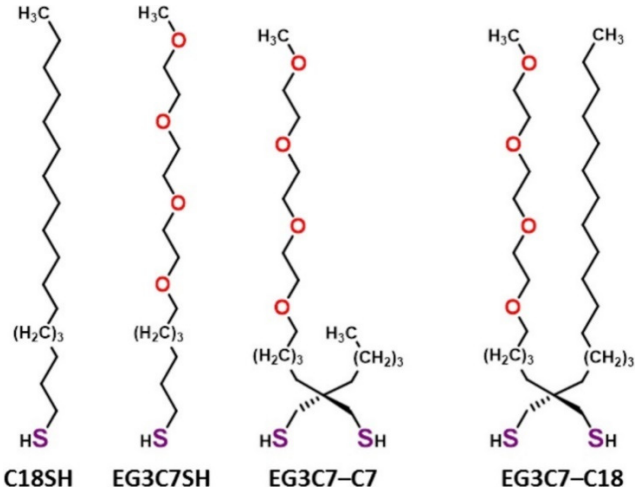

Figure 11. Structure of the unsymmetrical oligo(ethylene glycol) spiroalkanedithiols and their corresponding monodentate thiols [25]. Copyright 2017 American Chemical Society.

Moreover, the same research group examined the protein resistance of the unsymmetrical spiroalkanedithiol monolayers and compared the antifouling performance with the mono-alkanethiol and OEG-terminated alkanethiol SAMs using ellipsometric measurements. The results showed that the SAMs derived from double chains (EG3C7-C7 and EG3C7-C18) exhibited a moderate ability to inhibit fibrinogen adsorption but were not superior to EG3C7SH films [36]. Gudipati et al. first introduced an amphiphilic coating that was composed of hyperbranched fluoropolymer (HBFP) and PEG prepared on a self-assembled 3-aminopropyltriethoxysilane-functionalized microscope glass slide [95]. The behavior of HBFP-PEG coatings against the adsorption of proteins and lipopolysaccharides (bovine serum albumin (BSA), a lectin from *Codium fragile* (CFL), and lipopolysaccharides from *E. coli* (LPSE) and *Salmonella minnesota* (LPSS)) was investigated and compared with HBFP and PEG surfaces. The adsorption amounts of BSA and CFL were higher on the HBFP surface than on the PEG coating, while 100% surface coverage of LPSE and LPSS was achieved on the PEG coating and less than 20% coverage was observed on the HBFP surface. Interestingly, the amphiphilic HBFP-PEG coating was the most effective in repelling both protein and lipopolysaccharide adsorption.

In 2013, Li et al. studied the protein adsorption and cell adhesion of binary SAMs composed of perfluoroalkyl (PFA) and OEG alkanethiols (Figure 12) [69]. In the study, the adsorptions of three proteins (BSA, Fib, and IgG) on SAMs with different PFA/OEG ratio compositions were characterized by SPR (Figure 13 left). The three proteins exhibited similar behaviors on the surfaces and the data showed that the adsorption of proteins on the surface that was composed of 38% PFA was the most effective resistance (<5 ng cm^{-2}). Based on the results, it was proposed that the hydrophobic portions of the 38% PFA surface fail to match the hydrophobic patches on the protein, whereas the hydrophobic portions of the 74% PFA surface match well with those of the proteins. In addition to protein adsorption, HeLa cell adhesion after 24 h on the SAMs was investigated with an inverted fluorescence microscope (Figure 13 right). The number of adhered cells on the 38% PFA film was extremely small compared to the surface of the 74% and 85% PFA SAMs, which corresponded well to the data on protein adsorption.

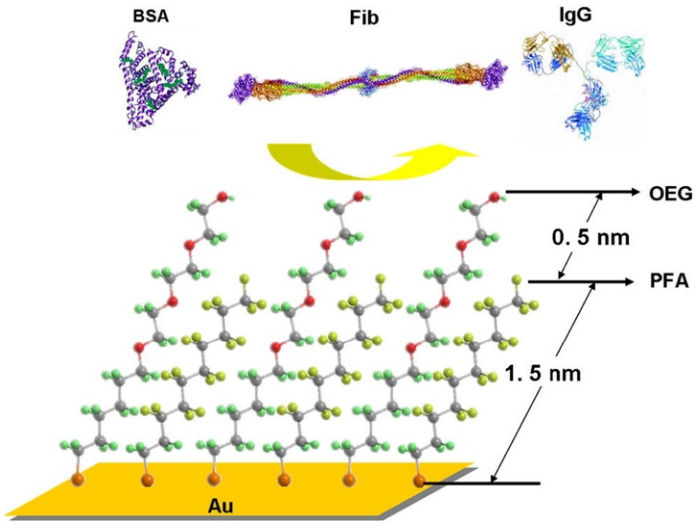

Figure 12. Illustration of amphiphilic binary SAMs on gold and three proteins (BSA, Fib, and IgG) [69]. Copyright 2013 Elsevier Inc.

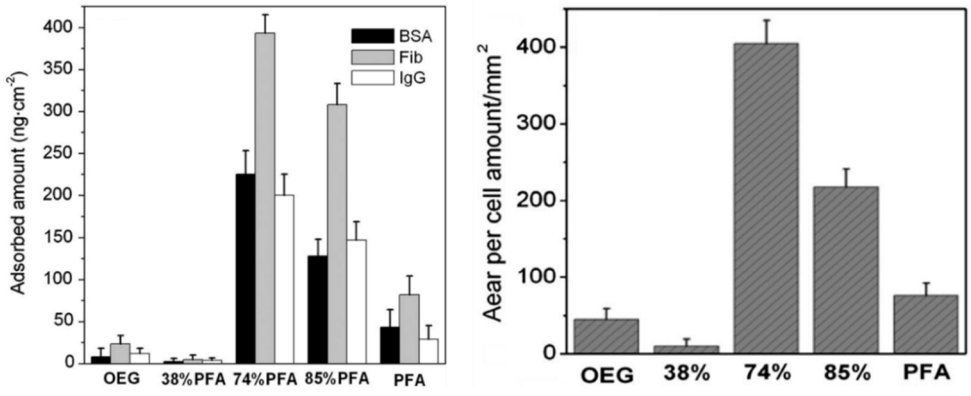

Figure 13. Protein (BSA, IgG, and Fib) adsorption (**left**) and cell adhesion (**right**) on amphiphilic binary SAMs with different PFA fractions [69]. Copyright 2013 Elsevier Inc.

5. Conclusions and Perspectives

The advance of antifouling coatings using SAMs on gold and silica surfaces against biomaterials has undergone significant progress in several decades. With this review, an attempt was made to briefly summarize the construction of antifouling surfaces, their characterizations, and their biomaterials resistance mechanisms based on their surface properties: hydrophobic, hydrophilic, and binary amphiphilic properties. The formation

of monolayers from hydrophilic moieties (such as OEG, zwitterion, or peptide) is undoubtedly a common approach to inhibit biofouling relying on a strong hydration layer. Furthermore, hydrophobic SAMs have been widely used for the fouling release method due to their low surface energy property. However, a single component of a surface coating with only hydrophobic or hydrophilic molecules might not be efficient for addressing all environmental complexities. Thus, the mixed hydrophobic/hydrophilic coating can be a promising candidate as an antifouling coating by adapting both antifouling and fouling release approaches. In this respect, our research group has investigated the generation of SAMs composed of phase-incompatible chemical moieties or other types of dissimilar molecular structures using bifunctional moieties [23–25,35,36,57,96–98]. These newly developed molecules, the use of thermally, hydrolytically, chemically, oxidatively, and electrochemically stable *N*-heterocyclic carbene headgroups [33,34,99], and innovative SAM-based strategies will undoubtedly pave the way for advances in surface modification for antifouling applications.

Author Contributions: Conceptualization, Y.C., H.-V.T., and T.R.L.; methodology, Y.C. and H.-V.T.; validation, H.-V.T.; formal analysis, Y.C.; writing—original draft preparation, Y.C.; writing—review and editing, Y.C., H.-V.T., and T.R.L.; visualization, Y.C. and H.-V.T.; supervision, T.R.L.; project administration, H.-V.T.; funding acquisition, T.R.L. All authors have read and agreed to the published version of the manuscript.

Funding: The authors are grateful for financial support from the National Science Foundation (CHE-2109174), the Robert A. Welch Foundation (Grant No. E-1320), and the Texas Center for Superconductivity at the University of Houston.

Institutional Review Board Statement: Not applicable.

Informed Consent Statement: Not applicable.

Data Availability Statement: Not applicable.

Conflicts of Interest: The authors declare no conflict of interest.

References

1. Zhou, F. *Antifouling Surfaces and Materials: From Land to Marine Environment*; Springer: Berlin, Germany, 2015; pp. 31–54.
2. Ahn, H.S.; Kim, K.M.; Lim, S.T.; Lee, C.H.; Han, S.W.; Choi, H.; Koo, S.; Kim, N.; Jerng, D.-W.; Wongwises, S. Anti-Fouling Performance of Chevron Plate Heat Exchanger by the Surface Modification. *Int. J. Heat Mass Transf.* **2019**, *144*, 118634. [CrossRef]
3. Scurria, A.; Scolaro, C.; Sfameni, S.; Di Carlo, G.; Pagliaro, M.; Visco, A.; Ciriminna, R. Towards AquaSun Practical Utilization: Strong Adhesion and Lack of Ecotoxicity of Solar-Driven Antifouling Sol-Gel Coating. *Prog. Org. Coat.* **2022**, *165*, 106771. [CrossRef]
4. Li, M.; Zhao, R.; Ma, S. Preparation of an Anti-Fouling Silicone Polyacrylate/SiO_2/HDPE Composite for Industrial Wastewater Pipe. *Mater. Lett.* **2021**, *304*, 130661. [CrossRef]
5. Bai, Z.; Wang, L.; Liu, C.; Yang, C.; Lin, G.; Liu, S.; Jia, K.; Liu, X. Interfacial Coordination Mediated Surface Segregation of Halloysite Nanotubes to Construct a High-Flux Antifouling Membrane for Oil-Water Emulsion Separation. *J. Membr. Sci.* **2021**, *620*, 118828. [CrossRef]
6. Song, Z.; Ma, Y.; Chen, M.; Ambrosi, A.; Ding, C.; Luo, X. Electrochemical Biosensor with Enhanced Antifouling Capability for COVID-19 Nucleic Acid Detection in Complex Biological Media. *Anal. Chem.* **2021**, *93*, 5963–5971. [CrossRef]
7. Lee, D.U.; Kim, D.W.; Lee, S.Y.; Choi, D.Y.; Choi, S.Y.; Moon, K.-S.; Shon, M.Y.; Moon, M.J. Amino Acid-Mediated Negatively Charged Surface Improve Antifouling and Tribological Characteristics for Medical Applications. *Colloids Surf. B Biointerfaces* **2022**, *211*, 112314. [CrossRef]
8. Yeginbayeva, I.A.; Atlar, M. An Experimental Investigation into the Surface and Hydrodynamic Characteristics of Marine Coatings with Mimicked Hull Roughness Ranges. *Biofouling* **2018**, *34*, 1001–1019. [CrossRef]
9. Qiu, H.; Feng, K.; Gapeeva, A.; Meurisch, K.; Kaps, S.; Li, X.; Yu, L.; Mishra, Y.K.; Adelung, R.; Baum, M. Functional Polymer Materials for Modern Marine Biofouling Control. *Prog. Polym. Sci.* **2022**, *127*, 101516. [CrossRef]
10. Damodaran, V.B.; Murthy, N.S. Bio-Inspired Strategies for Designing Antifouling Biomaterials. *Biomater. Res.* **2016**, *20*, 18. [CrossRef]
11. Magill, S.S.; Edwards, J.R.; Bamberg, W.; Beldavs, Z.G.; Dumyati, G.; Kainer, M.A.; Lynfield, R.; Maloney, M.; McAllister-Hollod, L.; Nadle, J.; et al. Multistate Point-Prevalence Survey of Health Care–Associated Infections. *N. Engl. J. Med.* **2014**, *370*, 1198–1208. [CrossRef]
12. Zhang, S.; Geryak, R.; Geldmeier, J.; Kim, S.; Tsukruk, V.V. Synthesis, Assembly, and Applications of Hybrid Nanostructures for Biosensing. *Chem. Rev.* **2017**, *117*, 12942–13038. [CrossRef] [PubMed]

13. Krsmanovic, M.; Biswas, D.; Ali, H.; Kumar, A.; Ghosh, R.; Dickerson, A.K. Hydrodynamics and Surface Properties Influence Biofilm Proliferation. *Adv. Colloid Interface Sci.* **2021**, *288*, 102336. [CrossRef] [PubMed]
14. Pradhan, S.; Kumar, S.; Mohanty, S.; Nayak, S.K. Environmentally Benign Fouling-Resistant Marine Coatings: A Review. Polym.-Plast. Technol. Mater. 2019, 58, 498–518. [CrossRef]
15. Zhang, H.; Chiao, M. Anti-Fouling Coatings of Poly(dimethylsiloxane) Devices for Biological and Biomedical Applications. *J. Med. Biol. Eng.* **2015**, *35*, 143–155. [CrossRef] [PubMed]
16. Brash, J.L.; Horbett, T.A.; Latour, R.A.; Tengvall, P. The Blood Compatibility Challenge. Part 2: Protein Adsorption Phenomena Governing Blood Reactivity. *Acta Biomater.* **2019**, *94*, 11–24. [CrossRef] [PubMed]
17. Uneputty, A.; Dávila-Lezama, A.; Garibo, D.; Oknianska, A.; Bogdanchikova, N.; Hernández-Sánchez, J.F.; Susarrey-Arce, A. Strategies Applied to Modify Structured and Smooth Surfaces: A Step Closer to Reduce Bacterial Adhesion and Biofilm Formation. *Colloids Interface Sci. Commun.* **2022**, *46*, 100560. [CrossRef]
18. Schøyen, M.; Green, N.W.; Hjermann, D.Ø.; Tveiten, L.; Beylich, B.; Øxnevad, S.; Beyer, J. Levels and Trends of Tributyltin (TBT) and Imposex in Dogwhelk (*Nucella lapillus*) along the Norwegian Coastline from 1991 to 2017. *Mar. Environ. Res.* **2019**, *144*, 1–8. [CrossRef]
19. Amara, I.; Miled, W.; Slama, R.B.; Ladhari, N. Antifouling Processes and Toxicity Effects of Antifouling Paints on Marine Environment. *A Review. Environ. Toxicol. Pharmacol.* **2018**, *57*, 115–130. [CrossRef]
20. Liu, B.; Liu, X.; Shi, S.; Huang, R.; Su, R.; Qi, W.; He, Z. Design and Mechanisms of Antifouling Materials for Surface Plasmon Resonance Sensors. *Acta Biomater.* **2016**, *40*, 100–118. [CrossRef]
21. Martins, S.E.; Fillmann, G.; Lillicrap, A.; Thomas, K.V. Review: Ecotoxicity of Organic and Organo-Metallic Antifouling Co-Biocides and Implications for Environmental Hazard and Risk Assessments in Aquatic Ecosystems. *Biofouling* **2018**, *34*, 34–52. [CrossRef]
22. Tian, L.; Yin, Y.; Bing, W.; Jin, E. Antifouling Technology Trends in Marine Environmental Protection. *J. Bionic Eng.* **2021**, *18*, 239–263. [CrossRef]
23. Sakunkaewkasem, S.; Marquez, M.D.; Lee, H.J.; Lee, T.R. Mixed Phase-Incompatible Monolayers: Toward Nanoscale Anti-Adhesive Coatings. *ACS Appl. Nano Mater.* **2020**, *3*, 4091–4101. [CrossRef]
24. Lee, H.J.; Jamison, A.C.; Lee, T.R. Two Are Better than One: Bidentate Adsorbates Offer Precise Control of Interfacial Composition and Properties. *Chem. Mater.* **2016**, *28*, 5356–5364. [CrossRef]
25. Chinwangso, P.; Lee, H.J.; Jamison, A.C.; Marquez, M.D.; Park, C.S.; Lee, T.R. Structure, Wettability, and Thermal Stability of Organic Thin-Films on Gold Generated from the Molecular Self-Assembly of Unsymmetrical Oligo(ethylene glycol) Spiroalkanedithiols. *Langmuir* **2017**, *33*, 1751–1762. [CrossRef] [PubMed]
26. Hasan, A.; Saxena, V.; Pandey, L.M. Surface Functionalization of Ti6Al4V via Self-Assembled Monolayers for Improved Protein Adsorption and Fibroblast Adhesion. *Langmuir* **2018**, *34*, 3494–3506. [CrossRef] [PubMed]
27. Qiang, Y.; Fu, S.; Zhang, S.; Chen, S.; Zou, X. Designing and Fabricating of Single and Double Alkyl-Chain Indazole Derivatives Self-Assembled Monolayer for Corrosion Inhibition of Copper. *Corros. Sci.* **2018**, *140*, 111–121. [CrossRef]
28. Yoon, H.J.; Liao, K.-C.; Lockett, M.R.; Kwok, S.W.; Baghbanzadeh, M.; Whitesides, G.M. Rectification in Tunneling Junctions: 2,2′-Bipyridyl-Terminated n-Alkanethiolates. *J. Am. Chem. Soc.* **2014**, *136*, 17155–17162. [CrossRef]
29. Macchia, E.; Tiwari, A.; Manoli, K.; Holzer, B.; Ditaranto, N.; Picca, R.A.; Cioffi, N.; Di Franco, C.; Scamarcio, G.; Palazzo, G.; et al. Label-Free and Selective Single-Molecule Bioelectronic Sensing with a Millimeter-Wide Self-Assembled Monolayer of Anti-Immunoglobulins. *Chem. Mater.* **2019**, *31*, 6476–6483. [CrossRef]
30. Jiang, C.; Wang, G.; Hein, R.; Liu, N.; Luo, X.; Davis, J.J. Antifouling Strategies for Selective In Vitro and In Vivo Sensing. *Chem. Rev.* **2020**, *120*, 3852–3889. [CrossRef]
31. Acosta, S.; Quintanilla, L.; Alonso, M.; Aparicio, C.; Rodríguez-Cabello, J.C. Recombinant AMP/Polypeptide Self-Assembled Monolayers with Synergistic Antimicrobial Properties for Bacterial Strains of Medical Relevance. *ACS Biomater. Sci. Eng.* **2019**, *5*, 4708–4716. [CrossRef]
32. Jakobi, V.; Schwarze, J.; Finlay, J.A.; Nolte, K.A.; Spöllmann, S.; Becker, H.-W.; Clare, A.S.; Rosenhahn, A. Amphiphilic Alginates for Marine Antifouling Applications. *Biomacromolecules* **2018**, *19*, 402–408. [CrossRef]
33. Crudden, C.M.; Horton, J.H.; Ebralidze, I.I.; Zenkina, O.V.; McLean, A.B.; Drevniok, B.; She, Z.; Kraatz, H.-B.; Mosey, N.J.; Seki, T.; et al. Ultra Stable Self-Assembled Monolayers of N-Heterocyclic Carbenes on Gold. *Nat. Chem.* **2014**, *6*, 409–414. [CrossRef] [PubMed]
34. Li, Z.; Narouz, M.R.; Munro, K.; Hao, B.; Crudden, C.M.; Horton, J.H.; Hao, H. Carboxymethylated Dextran-Modified N-Heterocyclic Carbene Self-Assembled Monolayers on Gold for Use in Surface Plasmon Resonance Biosensing. *ACS Appl. Mater. Interfaces* **2017**, *9*, 39223–39234. [CrossRef] [PubMed]
35. St. Hill, L.R.; Craft, J.W.; Chinwangso, P.; Tran, H.-V.; Marquez, M.D.; Lee, T.R. Antifouling Coatings Generated from Unsymmetrical Partially Fluorinated Spiroalkanedithiols. *ACS Appl. Bio Mater.* **2021**, *4*, 1563–1572. [CrossRef]
36. St. Hill, L.R.; Tran, H.-V.; Chinwangso, P.; Lee, H.J.; Marquez, M.D.; Craft, J.W.; Lee, T.R. Antifouling Studies of Unsymmetrical Oligo(ethylene glycol) Spiroalkanedithiol Self-Assembled Monolayers. *Micro* **2021**, *1*, 12. [CrossRef]
37. Wang, Y.-S.; Yau, S.; Chau, L.-K.; Mohamed, A.; Huang, C.-J. Functional Biointerfaces Based on Mixed Zwitterionic Self-Assembled Monolayers for Biosensing Applications. *Langmuir* **2019**, *35*, 1652–1661. [CrossRef] [PubMed]

38. Goda, T.; Tabata, M.; Sanjoh, M.; Uchimura, M.; Iwasaki, Y.; Miyahara, Y. Thiolated 2-Methacryloyloxyethyl Phosphorylcholine for an Antifouling Biosensor Platform. *Chem. Commun.* **2013**, *49*, 8683–8685. [CrossRef] [PubMed]
39. Koc, J.; Schardt, L.; Nolte, K.; Beyer, C.; Eckhard, T.; Schwiderowski, P.; Clarke, J.L.; Finlay, J.A.; Clare, A.S.; Muhler, M.; et al. Effect of Dipole Orientation in Mixed, Charge-Equilibrated Self-Assembled Monolayers on Protein Adsorption and Marine Biofouling. *ACS Appl. Mater. Interfaces* **2020**, *12*, 50953–50961. [CrossRef] [PubMed]
40. Ostuni, E.; Yan, L.; Whitesides, G.M. The Interaction of Proteins and Cells with Self-Assembled Monolayers of Alkanethiolates on Gold and Silver. *Colloids Surf. B Biointerfaces* **1999**, *15*, 3–30. [CrossRef]
41. Höök, F.; Vörös, J.; Rodahl, M.; Kurrat, R.; Böni, P.; Ramsden, J.J.; Textor, M.; Spencer, N.D.; Tengvall, P.; Gold, J.; et al. A Comparative Study of Protein Adsorption on Titanium Oxide Surfaces Using in Situ Ellipsometry, Optical Waveguide Lightmode Spectroscopy, and Quartz Crystal Microbalance/Dissipation. *Colloids Surf. B Biointerfaces* **2002**, *24*, 155–170. [CrossRef]
42. Rabe, M.; Verdes, D.; Seeger, S. Understanding Protein Adsorption Phenomena at Solid Surfaces. *Adv. Colloid Interface Sci.* **2011**, *162*, 87–106. [CrossRef]
43. Elwing, H. Protein Absorption and Ellipsometry in Biomaterial Research. *Biomaterials* **1998**, *19*, 397–406. [CrossRef]
44. Ostuni, E.; Chapman, R.G.; Liang, M.N.; Meluleni, G.; Pier, G.; Ingber, D.E.; Whitesides, G.M. Self-Assembled Monolayers that Resist the Adsorption of Proteins and the Adhesion of Bacterial and Mammalian Cells. *Langmuir* **2001**, *17*, 6336–6343. [CrossRef]
45. Chapman, R.G.; Ostuni, E.; Yan, L.; Whitesides, G.M. Preparation of Mixed Self-Assembled Monolayers (SAMs) that Resist Adsorption of Proteins Using the Reaction of Amines with a SAM that Presents Interchain Carboxylic Anhydride Groups. *Langmuir* **2000**, *16*, 6927–6936. [CrossRef]
46. Prime, K.L.; Whitesides, G.M. Self-Assembled Organic Monolayers: Model Systems for Studying Adsorption of Proteins at Aurfaces. *Science* **1991**, *252*, 1164–1167. [CrossRef] [PubMed]
47. Harder, P.; Grunze, M.; Dahint, R.; Whitesides, G.M.; Laibinis, P.E. Molecular Conformation in Oligo(ethylene glycol)-Terminated Self-Assembled Monolayers on Gold and Silver Surfaces Determines their Ability To Resist Protein Adsorption. *J. Phys. Chem. B* **1998**, *102*, 426–436. [CrossRef]
48. Li, L.; Chen, S.; Zheng, J.; Ratner, B.D.; Jiang, S. Protein Adsorption on Oligo(ethylene glycol)-Terminated Alkanethiolate Self-Assembled Monolayers: The Molecular Basis for Nonfouling Behavior. *J. Phys. Chem. B* **2005**, *109*, 2934–2941. [CrossRef]
49. Prime, K.L.; Whitesides, G.M. Adsorption of Proteins onto Surfaces Containing End-Attached Oligo(ethylene oxide): A Model System Using Self-Assembled Monolayers. *J. Am. Chem. Soc.* **1993**, *115*, 10714–10721. [CrossRef]
50. Herrwerth, S.; Eck, W.; Reinhardt, S.; Grunze, M. Factors that Determine the Protein Resistance of Oligoether Self-Assembled Monolayers-Internal Hydrophilicity, Terminal Hydrophilicity, and Lateral Packing Density. *J. Am. Chem. Soc.* **2003**, *125*, 9359–9366. [CrossRef]
51. Holmlin, R.E.; Chen, X.; Chapman, R.G.; Takayama, S.; Whitesides, G.M. Zwitterionic SAMs that Resist Nonspecific Adsorption of Protein from Aqueous Buffer. *Langmuir* **2001**, *17*, 2841–2850. [CrossRef]
52. Huang, C.-J.; Chu, S.-H.; Li, C.-H.; Lee, T.R. Surface Modification with Zwitterionic Cysteine Betaine for Nanoshell-Assisted Near-Infrared Plasmonic Hyperthermia. *Colloids Surf. B Biointerfaces* **2016**, *145*, 291–300. [CrossRef]
53. Luk, Y.-Y.; Kato, M.; Mrksich, M. Self-Assembled Monolayers of Alkanethiolates Presenting Mannitol Groups are Inert to Protein Adsorption and Cell Attachment. *Langmuir* **2000**, *16*, 9604–9608. [CrossRef]
54. Ostuni, E.; Chapman, R.G.; Holmlin, R.E.; Takayama, S.; Whitesides, G.M. A Survey of Structure-Property Relationships of Surfaces that Resist the Adsorption of Protein. *Langmuir* **2001**, *17*, 5605–5620. [CrossRef]
55. Chen, S.; Yu, F.; Yu, Q.; He, Y.; Jiang, S. Strong Resistance of a Thin Crystalline Layer of Balanced Charged Groups to Protein Adsorption. *Langmuir* **2006**, *22*, 8186–8191. [CrossRef] [PubMed]
56. Chen, S.; Zheng, J.; Li, L.; Jiang, S. Strong Resistance of Phosphorylcholine Self-Assembled Monolayers to Protein Adsorption: Insights into Nonfouling Properties of Zwitterionic Materials. *J. Am. Chem. Soc.* **2005**, *127*, 14473–14478. [CrossRef]
57. Huang, C.-J.; Chu, S.-H.; Wang, L.-C.; Li, C.-H.; Lee, T.R. Bioinspired Zwitterionic Surface Coatings with Robust Photostability and Fouling Resistance. *ACS Appl. Mater. Interfaces* **2015**, *7*, 23776–23786. [CrossRef]
58. Humblot, V.; Yala, J.-F.; Thebault, P.; Boukerma, K.; Héquet, A.; Berjeaud, J.-M.; Pradier, C.-M. The Antibacterial Activity of Magainin I Immobilized onto Mixed Thiols Self-Assembled Monolayers. *Biomaterials* **2009**, *30*, 3503–3512. [CrossRef]
59. Nowinski, A.K.; Sun, F.; White, A.D.; Keefe, A.J.; Jiang, S. Sequence, Structure, and Function of Peptide Self-Assembled Monolayers. *J. Am. Chem. Soc.* **2012**, *134*, 6000–6005. [CrossRef]
60. Fyrner, T.; Lee, H.-H.; Mangone, A.; Ekblad, T.; Pettitt, M.E.; Callow, M.E.; Callow, J.A.; Conlan, S.L.; Mutton, R.; Clare, A.S.; et al. Saccharide-Functionalized Alkanethiols for Fouling-Resistant Self-Assembled Monolayers: Synthesis, Monolayer Properties, and Antifouling Behavior. *Langmuir* **2011**, *27*, 15034–15047. [CrossRef]
61. Siegers, C.; Biesalski, M.; Haag, R. Self-Assembled Monolayers of Dendritic Polyglycerol Derivatives on Gold that Resist the Adsorption of Proteins. *Chem. Eur. J.* **2004**, *10*, 2831–2838. [CrossRef]
62. Callow, J.A.; Callow, M.E.; Ista, L.K.; Lopez, G.; Chaudhury, M.K. The Influence of Surface Energy on the Wetting Behaviour of the Spore Adhesive of the Marine Alga *Ulva linza* (Synonym *Enteromorpha linza*). *J. R. Soc. Interface* **2005**, *2*, 319–325. [CrossRef]
63. Khan, M.M.T.; Ista, L.K.; Lopez, G.P.; Schuler, A.J. Experimental and Theoretical Examination of Surface Energy and Adhesion of Nitrifying and Heterotrophic Bacteria Using Self-Assembled Monolayers. *Environ. Sci. Technol.* **2011**, *45*, 1055–1060. [CrossRef] [PubMed]

64. Lehnfeld, J.; Dukashin, Y.; Mark, J.; White, G.D.; Wu, S.; Katzur, V.; Müller, R.; Ruhl, S. Saliva and Serum Protein Adsorption on Chemically Modified Silica Surfaces. *J. Dent. Res.* **2021**, *100*, 1047–1054. [CrossRef] [PubMed]
65. Kim, D.J.; Lee, J.M.; Park, J.-G.; Chung, B.G. A Self-Assembled Monolayer-Based Micropatterned Array for Controlling Cell Adhesion and Protein Adsorption. *Biotechnol. Bioeng.* **2011**, *108*, 1194–1202. [CrossRef] [PubMed]
66. Pranzetti, A.; Salaün, S.; Mieszkin, S.; Callow, M.E.; Callow, J.A.; Preece, J.A.; Mendes, P.M. Model Organic Surfaces to Probe Marine Bacterial Adhesion Kinetics by Surface Plasmon Resonance. *Adv. Funct. Mater.* **2012**, *22*, 3672–3681. [CrossRef]
67. Faucheux, N.; Schweiss, R.; Lützow, K.; Werner, C.; Groth, T. Self-Assembled Monolayers with Different Terminating Groups as Model Substrates for Cell Adhesion Studies. *Biomaterials* **2004**, *25*, 2721–2730. [CrossRef]
68. Patel, K.R.; Tang, H.; Grever, W.E.; Simon Ng, K.Y.; Xiang, J.; Keep, R.F.; Cao, T.; McAllister, J.P. Evaluation of Polymer and Self-Assembled Monolayer-Coated Silicone Surfaces to Reduce Neural Cell Growth. *Biomaterials* **2006**, *27*, 1519–1526. [CrossRef]
69. Li, S.; Yang, D.; Tu, H.; Deng, H.; Du, D.; Zhang, A. Protein Adsorption and Cell Adhesion Controlled by the Surface Chemistry of Binary Perfluoroalkyl/Oligo(ethylene glycol) Self-Assembled Monolayers. *J. Colloid Interface Sci.* **2013**, *402*, 284–290. [CrossRef]
70. Yang, Z.; Galloway, J.A.; Yu, H. Protein Interactions with Poly(ethylene glycol) Self-Assembled Monolayers on Glass Substrates: Diffusion and Adsorption. *Langmuir* **1999**, *15*, 8405–8411. [CrossRef]
71. Feldman, K.; Hähner, G.; Spencer, N.D.; Harder, P.; Grunze, M. Probing Resistance to Protein Adsorption of Oligo(ethylene glycol)-Terminated Self-Assembled Monolayers by Scanning Force Microscopy. *J. Am. Chem. Soc.* **1999**, *121*, 10134–10141. [CrossRef]
72. Lan, S.; Veiseh, M.; Zhang, M. Surface Modification of Silicon and Gold-Patterned Silicon Surfaces for Improved Biocompatibility and Cell Patterning Selectivity. *Biosens. Bioelectron.* **2005**, *20*, 1697–1708. [CrossRef]
73. Jeon, S.I.; Lee, J.H.; Andrade, J.D.; De Gennes, P.G. Protein—Surface Interactions in the Presence of Polyethylene Oxide: I. *Simplified Theory. J. Colloid Interface Sci.* **1991**, *142*, 149–158. [CrossRef]
74. Latour, R.A. Fundamental Principles of the Thermodynamics and Kinetics of Protein Adsorption to Material Surfaces. *Colloids Surf. B Biointerfaces* **2020**, *191*, 110992. [CrossRef] [PubMed]
75. Pertsin, A.J.; Grunze, M. Computer Simulation of Water near the Surface of Oligo(ethylene glycol)-Terminated Alkanethiol Self-Assembled Monolayers. *Langmuir* **2000**, *16*, 8829–8841. [CrossRef]
76. Pertsin, A.J.; Hayashi, T.; Grunze, M. Grand Canonical Monte Carlo Simulations of the Hydration Interaction between Oligo(ethylene glycol)-Terminated Alkanethiol Self-Assembled Monolayers. *J. Phys. Chem. B* **2002**, *106*, 12274–12281. [CrossRef]
77. Shao, Q.; Jiang, S. Molecular Understanding and Design of Zwitterionic Materials. *Adv. Mater.* **2015**, *27*, 15–26. [CrossRef]
78. Chen, S.; Li, L.; Zhao, C.; Zheng, J. Surface Hydration: Principles and Applications toward Low-Fouling/Nonfouling Biomaterials. *Polymer* **2010**, *51*, 5283–5293. [CrossRef]
79. Liu, S.; Tang, J.; Ji, F.; Lin, W.; Chen, S. Recent Advances in Zwitterionic Hydrogels: Preparation, Property, and Biomedical Application. *Gels* **2022**, *8*, 46. [CrossRef]
80. Ishihara, K.; Nomura, H.; Mihara, T.; Kurita, K.; Iwasaki, Y.; Nakabayashi, N. Why Do Phospholipid Polymers Reduce Protein Adsorption? *J. Biomed. Mater. Res.* **1998**, *39*, 323–330. [CrossRef]
81. Shao, Q.; Jiang, S. Influence of Charged Groups on the Properties of Zwitterionic Moieties: A Molecular Simulation Study. *J. Phys. Chem. B* **2014**, *118*, 7630–7637. [CrossRef]
82. Amit, M.; Yuran, S.; Gazit, E.; Reches, M.; Ashkenasy, N. Tailor-Made Functional Peptide Self-Assembling Nanostructures. *Adv. Mater.* **2018**, *30*, 1707083. [CrossRef]
83. Hower, J.C.; He, Y.; Bernards, M.T.; Jiang, S. Understanding the Nonfouling Mechanism of Surfaces through Molecular Simulations of Sugar-Based Self-Assembled Monolayers. *J. Chem. Phys.* **2006**, *125*, 214704. [CrossRef] [PubMed]
84. Nurioglu, A.G.; Esteves, A.C.C.; de With, G. Non-Toxic, Non-Biocide-Release Antifouling Coatings Based on Molecular Structure Design for Marine Applications. *J. Mater. Chem. B* **2015**, *3*, 6547–6570. [CrossRef] [PubMed]
85. Baier, R.E. Surface Behaviour of Biomaterials: The *Theta Surface* for Biocompatibility. *J. Mater. Sci.: Mater. Med.* **2006**, *17*, 1057–1062. [CrossRef] [PubMed]
86. Shafrin, E.G.; Zisman, W.A. Critical Surface Tension for Spreading on a Liquid Substrate. *J. Phys. Chem.* **1967**, *71*, 1309–1316. [CrossRef]
87. Schrader, M.E. On Adhesion of Biological Substances to Low Energy Solid Surfaces. *J. Colloid Interface Sci.* **1982**, *88*, 296–297. [CrossRef]
88. Ostuni, E.; Grzybowski, B.A.; Mrksich, M.; Roberts, C.S.; Whitesides, G.M. Adsorption of Proteins to Hydrophobic Sites on Mixed Self-Assembled Monolayers. *Langmuir* **2003**, *19*, 1861–1872. [CrossRef]
89. Li, Y.; Gao, Y.H.; Li, X.S.; Yang, J.Y.; Que, G.H. Influence of Surface Free Energy on the Adhesion of Marine Benthic Diatom *Nitzschia Closterium* MMDL533. *Colloids Surf. B Biointerfaces* **2010**, *75*, 550–556. [CrossRef]
90. Zhang, Z.; Zhang, M.; Chen, S.; Horbett, T.A.; Ratner, B.D.; Jiang, S. Blood Compatibility of Surfaces with Superlow Protein Adsorption. *Biomaterials* **2008**, *29*, 4285–4291. [CrossRef]
91. Cheng, G.; Zhang, Z.; Chen, S.; Bryers, J.D.; Jiang, S. Inhibition of Bacterial Adhesion and Biofilm Formation on Zwitterionic Surfaces. *Biomaterials* **2007**, *28*, 4192–4199. [CrossRef]
92. Sperling, C.; Schweiss, R.B.; Streller, U.; Werner, C. In Vitro Hemocompatibility of Self-Assembled Monolayers Displaying Various Functional Groups. *Biomaterials* **2005**, *26*, 6547–6557. [CrossRef]
93. Brady, R.F., Jr.; Singer, I.L. Mechanical Factors Favoring Release from Fouling Release Coatings. *Biofouling* **2000**, *15*, 73–81. [CrossRef] [PubMed]

94. Callow, J.A.; Callow, M.E. Trends in the Development of Environmentally Friendly Fouling-Resistant Marine Coatings. *Nat. Commun.* **2011**, *2*, 244. [CrossRef] [PubMed]
95. Gudipati, C.S.; Finlay, J.A.; Callow, J.A.; Callow, M.E.; Wooley, K.L. The Antifouling and Fouling-Release Performance of Hyperbranched Fluoropolymer (HBFP)−Poly(ethylene glycol) (PEG) Composite Coatings Evaluated by Adsorption of Biomacromolecules and the Green Fouling Alga Ulva. *Langmuir* **2005**, *21*, 3044–3053. [CrossRef] [PubMed]
96. Chinwangso, P.; Lee, H.J.; Lee, T.R. Self-Assembled Monolayers Generated from Unsymmetrical Partially Fluorinated Spiroalkanedithiols. *Langmuir* **2015**, *31*, 13341–13349. [CrossRef] [PubMed]
97. Marquez, M.D.; Zenasni, O.; Jamison, A.C.; Lee, T.R. Homogeneously Mixed Monolayers: Emergence of Compositionally Conflicted Interfaces. *Langmuir* **2017**, *33*, 8839–8855. [CrossRef]
98. Chinwangso, P.; St. Hill, L.R.; Marquez, M.D.; Lee, T.R. Unsymmetrical Spiroalkanedithiols Having Mixed Fluorinated and Alkyl Tailgroups of Varying Length: Film Structure and Interfacial Properties. *Molecules* **2018**, *23*, 2632. [CrossRef]
99. Choi, Y.; Park, C.S.; Tran, H.-V.; Li, C.-H.; Crudden, C.M.; Lee, T.R. Functionalized N-Heterocyclic Carbene Monolayers on Gold for Surface-Initiated Polymerizations. *ACS Appl. Mater. Interfaces* **2022**. [CrossRef]